Characterization and Applications of Modulated Optical Nanoprobes (MOONs)

Jeffrey N. Anker[1], Caleb J. Behrend[1], Brandon H. McNaughton[1], Teresa Gail Roberts[1], Murphy Brasuel[2], Martin A. Philbert[3], and Raoul Kopelman[1]
[1]University of Michigan Chemistry Department, Ann Arbor, Michigan 48109-1055.
[2]Colarado College Chemistry Department, Colorado Springs, Colorado 80903.
[3]University of Michigan School of Public Health, Ann Arbor, Michigan 48109.

ABSTRACT
Modulated optical nanoprobes (MOONs) are microscopic (spherical and aspherical) particles designed to emit different fluxes of light in a manner that depends on particle orientation. When particle orientation is controlled remotely using magnetic fields (MagMOONs) it allows modulation of fluorescence intensity in any selected pattern including square and sinusoidal waves. The broad range of sizes over which MOONs can be prepared allows them to be tailored to applications from intracellular sensors using submicron MOONs to immunoassays using larger MOONs (1-10μm). In the absence of external fields, or material that responds to external fields, the particles tumble erratically due to Brownian thermal forces. These erratic changes in orientation cause the MOONs to blink. The temporal pattern of blinking contains information about the local rheological environment and any forces and torques acting on the MOONs.

INTRODUCTION
In order to visualize physical and chemical dynamics within microscopic environments and even within living cells, a variety of nanoprobes have recently been developed[1]. One type of sensor utilizes fluorescence indicator and reference dyes encapsulated in a polymer matrix to measure local chemical concentrations[2,3]. These nano-sensors have several advantages over conventional molecular probes: First, the polymer matrix protects the dye from interferences such as quenching due to protein binding. For instance, Xu et al. showed that addition of albumin protein far below physiological protein concentrations resulted in near saturation of response from an oxygen sensing fluorophore; however, encapsulation of the fluorophore reduced interference to a negligible level[4]. In the case of cellular applications, the encapsulation of the dye also protects the cell from potentially toxic effects. A second strength of nanoparticle sensors is that the matrix provides a separate sensing phase, distinct from the surrounding environment, allowing multi-component sensor and effector systems to be prepared. These systems include enzyme coupled[5] and ionophore coupled[6] fluorescent sensors, photodynamic effectors, MRI contrast enhancing agents, and molecularly targeted systems[1]. In addition to MRI enhancement, incorporation of magnetic material allows particles and swarms of particles to be guided and oriented with external magnetic field gradients and field directions[7-9].

Most fluorescent nanospheres and microspheres emit light uniformly in all directions. By carefully constructing nano-systems that emit anistropically, it becomes possible to monitor particle orientation, and to modulate the light emitted from the particles as they rotate[8-10]. Tracking the orientation of these modulated optical nanoprobes (MOONs) allows one to observe torques acting on the MOONs. These torques reveal much information about the MOONs and the properties of the environment

around them. By measuring the effect of these torques on particle fluorescence it becomes possible to measure visco-elastic properties, observe thermal fluctuations, measure molecular and physical interactions, and observe vorticity in fluid flow. Simultaneously, modulated optical signals stand out against the unmodulated background fluorescence, allowing more sensitive optical analysis in the presence of background.

We have prepared magnetically modulated optical nanoprobes (MagMOONs) where an external magnetic field orients the particles and causes them to blink synchronously in rotating magnetic fields[8,9]. In the absence of magnetic fields, or if the particles contain no magnetic material, the particles nevertheless rotate erratically due to thermal fluctuations (Browian MOONs)[10]. We have prepared MOONs ranging from 200nm to 5μm, and are developing smaller particles.

EXPERIMENTAL METHOD

MOONs can be prepared by coating one hemisphere of a particle with an opaque metal so that light is emitted only from the other hemisphere (moon shaped particles)[9,11]. A second type of MOON, aspherical MOONs, have aspherical shapes and emit different fluxes (and/or polarizations) of light from different geometric faces due to absorption and total internal reflection within the particle[8,12,13]. Here, we focus mainly on metal-capped MOONs.

Prior to metal-capping, microparticles and nanoparticles can be prepared by a variety of methods including inverse micelle polymerization[14], Stober synthesis[15], grinding larger polymer blocks into particles with a mortar and pestle[16], and ormosil formation.. The particles can subsequently be modified by chemically functionalizing their surfaces, "breading" them with fluorescent or magnetic nanocrumbs[8,12], or swelling them with dyes and ionophores[6].

Fluorescent polystyrene microspheres 4.4μm in diameter containing ferromagnetic material were purchased (Spherotech, Libertyville, IL). Fluorescent polystyrene spheres from 170nm to 3μm in diameter were purchased from Bangs Labs (Fishers, IN). Silica nanoparticles 300nm in diameter for pH sensitive MagMOONs were prepared as follows: Magnetic barium ferrite (BaM) crystals 30nm in diameter (a gift from Toda Kogyo Corp.) were ground for one hour in an aluminum oxide mortar and pestle. Approximately 200 mg of ground BaM were sonicated for one hour in 24 mL of an ethanol solution that contained 2M ammonia and 6M deionized water. After sonication, the suspension was centrifuged for 15 minutes at 500 RPM to remove aggregates. 24 mL of supernatant were transferred to a 100 mL round bottom flask. 800 μL of dextran linked SNARF pH indicator dye (5 mg dye per 1 mL deionized water) was added to the same flask. The polymerization reaction was initiated by adding 70 μL tetraethylorthosilicate (TEOS). The reaction was allowed to progress for 2 hours, after which the silica nanoparticles were removed by vacuum filtration.

A typical preparation method to make metal-capped MagMOONs is illustrated in Figure 1, and described as follows:

(i). We deposit a monolayer of microspheres or nanospheres containing permanent magnetic material onto a glass microscope slide: We disperse the magnetic microspheres/nanospheres in water or ethanol solution, and spread a drop of solution onto

a glass slide and let it dry. The magnetic orientation of the particles is irrelevant at this stage; if they have been magnetized at all, they can be remagnetized later.

(ii). Next, we place the microscope slide in either an aluminum vapor coater or a gold sputter coater. Aluminum vapor deposition is performed in a vacuum so the vaporized aluminum moves in a straight line (conservation of momentum) from the source to the target, thereby coating only one hemisphere of the particles and leaving the other hemisphere in shadow.

(iii). All the particles are now coated with metal on the same face, relative to the glass slide and to each other. We place the glass slide in a strong magnetic field to magnetize the particles. The glass slide is oriented in the magnetic field so that the metal capping becomes a south pole and the uncoated side becomes a north pole. At this point the microspheres are magnetized so that their north side is uncoated.

(iv). The MagMOONs keep very well on the metal-coated glass slide. They can be removed from the slide at any point using an artist's paintbrush. Sonicating the brush at 42 KHz for 20 seconds in aqueous solution suspends the particles.

(v) In an external magnetic field, all MagMOONs orient and align with in the direction of the field.

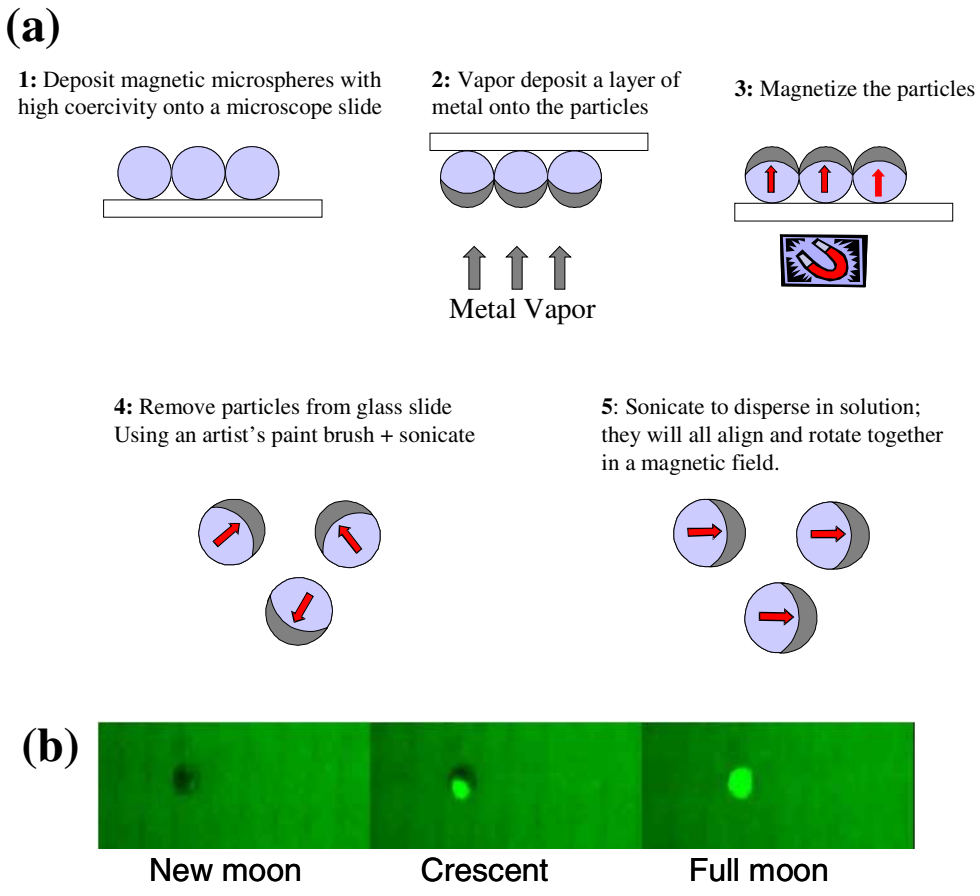

Figure 1 (a) Preparation of metal capped Modulated Optical Nanoprobes by vapor deposition. (b) Images of Brownian MOONs prepared by vacuum metalization. The fluorescent nanoprobes are shown in different orientations with a constant fluorescent background.

The preparation of Brownian MOONs is simpler than MagMOONs because no embedded magnetic nano-seeds are required, as well as no external magnetic fields. Brownian MOONs require steps 1, 2, and 4, whereas steps 3 and 5, magnetization and magnetic orientation respectively, are specific to MagMOONs.

The thickness of metal capping is determined first by using a piezo-electric thickness monitor during the vacuum deposition process. It can then be verified by measuring the percentage of light transmitted through the metal coating compared to an uncoated portion of the slide (Figure 2a) assuming a skin depth of 9nm for aluminum and 17nm for gold for light of wavelength 589nm[17]. Interestingly, the metal capping increases fluorescence intensity emitted from capped microspheres. This is illustrated in Figures 2b and 2c, where particles oriented towards the objective emit approximately 130% more light than the adjacent uncapped microspheres. This enhancement may arise from increased excitation pathlength as well as reflection towards the objective of fluorescence that would usually be emitted away from the objective.

The MagMOONs and Brownian MOONs were viewed with an Olympus IMT-II (Lake Success, NY, USA) inverted fluorescence microscope. Fluorescence spectra were acquired using an Acton Research Corp. spectrograph and a Hamamatsu HC230 CCD interfaced with an Intel Pentium computer. Images and videos of Brownian MOONs were acquired with a Nikon Coolpix 995 digital camera. To modulate MagMOONs, a permanent magnet is held above the microscope stage and rotated with a stepper motor attached to the magnet. A program written in LABVIEW (National Instruments, Austin, TX) controls the stepper motor with pulses sent through the parallel port. Spectra are acquired and saved after every rotation. The probe spectrum is calculated as the average "On minus Off" spectrum. MagMOON signals can also be modulated by switching the polarity of the current sent through an electromagnet to orient the particles on and off.

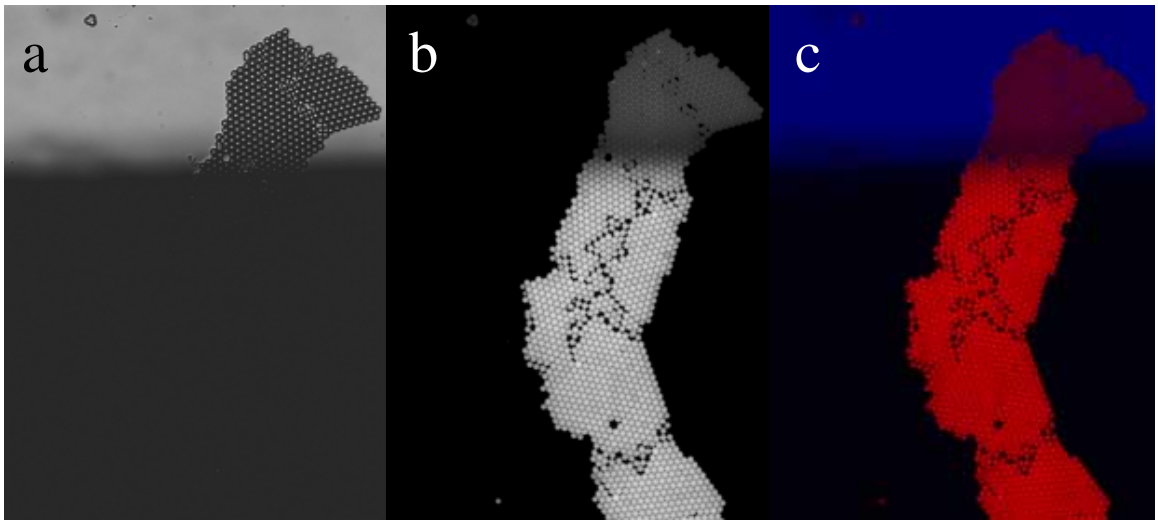

Figure 2. A monolayer aggregate of 3µm microspheres with aluminum coating on the bottom ¾ of the view. (a) Bright field image at the edge of the metal coating with high transmission on the top where the metal coating is absent. (b) Fluorescence from coated particles (bottom) and uncoated particles (top). The metal coating results in higher intensity fluorescence. (c) Overlaid bright field and fluorescence image.

Rat macrophages were cultured in Dulbecco's modified Eagle medium. Five days prior to sensor delivery and testing the cells were removed from the culture dishes using trypsin and plated on uncoated 22-mm glass covers slips. Twenty-four hours before observations were made, 50 microliters of Brownian MOONs in 10mM phosphate buffered saline were added to the culture media for each cover slip.

RESULTS AND DISCUSSION

Metal-capped MagMOONs need a relatively high coercivity in order to orient in a magnetic field and not be remagnetized by the field. The 4.4µm magnetic particles containing chromium dioxide shown in figures 1b, 3, and 4 have a coercivity of 570 ±10 Oe. By contrast, aspherical MagMOONs orient due to shape anisotropy, and need not have a high coercivity. For instance 1-2µm magnetic fluorescent microspheres (Polysciences) used to form chain-shaped aspherical MagMOONs[8] have a coercivity of only 27±2 Oe. The saturation magnetization of the particles provides a measure of the amount of magnetic material loaded into the microspheres. The Spherotech microspheres contained 18% chromium dioxide by mass, and the Polysciences contain 70% by mass.

MagMOON fluorescence is easily separated from background by orienting the particles "On" and "Off" a number of times, and subtracting "Off" from "On" spectra. Fluorescent 4.4µm aluminum-capped MagMOONs were prepared by metal capping and magnetizing fluorescent microspheres containing chromium dioxide (Spherotech, IL). The MagMOONs were dispersed in ovine albumin (egg white) and drop of the solution was placed on a microscope slide. The computer oriented the MagMOONs and acquired 32 pairs of "On" and "Off" spectra. Figure 4 illustrates how a yellow aluminum-capped MagMOON spectrum was separated from the 800nm light leaking from the mercury lamp, and from the green fluorescence of ovine albumin. Spectral subtraction reduced the background mercury lamp peak by a factor of 5,000 and rendered negligible the green albumin fluorescence. Using principal components analysis (PCA) further improves the separation of signal from background.

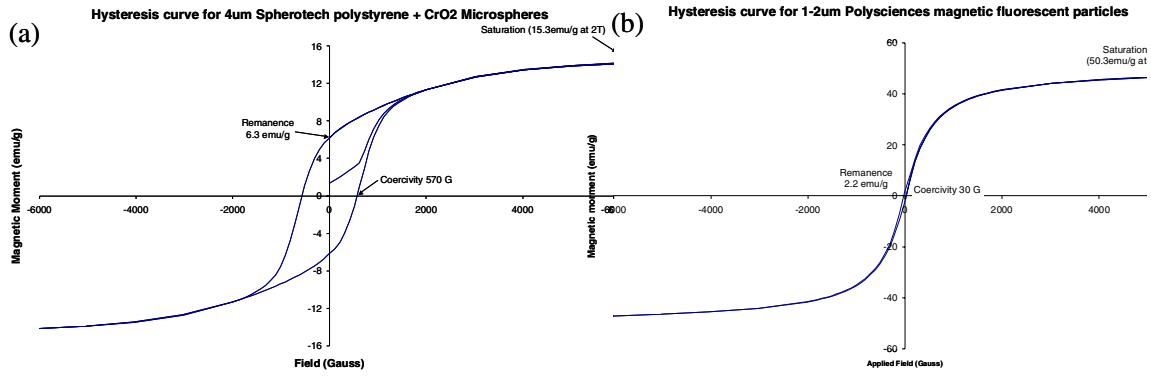

Figure 3. The hysteresis curve for (a) 4.4µm chromium dioxide containing polystyrene microspheres with high coercivity and (b) 1µm iron oxide containing polystyrene particles with low coercivity.

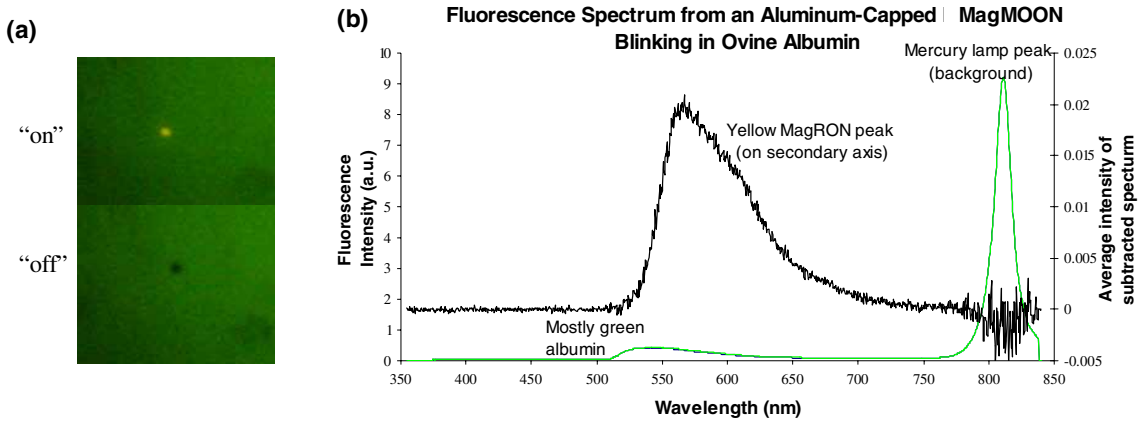

Figure 4. An aluminum-capped MagMOON blinking in ovine albumin (a medium with similar viscosity to cellular cytoplasm). (a)Images of a MagMOON oriented "On" and "Off." (b) Spectra of the MagMOON oriented "On" (green line) and "Off" (black line just below the green). Spectral subtraction reduced background at 800nm from mercury-lamp peak by a factor of 5,000 and rendered negligible the green albumin fluorescence. The "On minus Off" spectrum (black line peaking at 565nm) is plotted on the secondary axis on the right of the graph.

MagMOONs can be used for improved immunoassays. The surface of MagMOONs is first functionalized with molecular recognition elements, to which analyte binds and is labeled leading to a change in MagMOON fluorescence. By modulating MagMOONs, their emitted signal can be separated from the optical and electronic backgrounds, including autofluorescence and excess fluorescent dye not attached to the particle. Reducing background leads to more sensitive measurements and simpler analytical procedures or experimental protocols[8,9].

Initial demonstrations of MagMOONs used larger particles, approximately 4μm diameter microspheres or long chains of 1μm particles[8,9], although 300nm Brownian MOONs were also described[9]. In order to introduce MagMOONs into cells with minimal perturbation, it is necessary to reduce their size to submicron dimensions. We have produced pH sensitive 300nm MagMOONs. The MagMOONs consist of a silica matrix embedded with: barium ferrite nanoparticles to provide magnetic orientation, and dextran-linked SNARF (Molecular Probes, Eugene OR), a ratiometric pH sensitve dye. Figure 4 a) Shows the effect of pH on the fluorescence emission spectrum from a concentrated solution of MagMOONs. Figure 4 b) shows the "On" and "Off" spectrum from a single MagMOON in a solution with pH 5.5-6. The on and off spectra include optical and electronic backgrounds that are many times stronger than the MagMOON spectrum. The On and Off spectra overlap closely on the graph. Figure 4c) shows the "On" minus "Off" modulated MagMOON spectrum.

In the absence of external rotating magnetic fields, the only surviving rotational motion of the nanoparticles or nanospheres is due to Brownian motion (rotation). This is a new tool that makes it possible to study fundamental properties of soft materials, complex liquids, inhomogeneous liquids and liquid crystals, using restricted Brownian rotations (Figure 6).

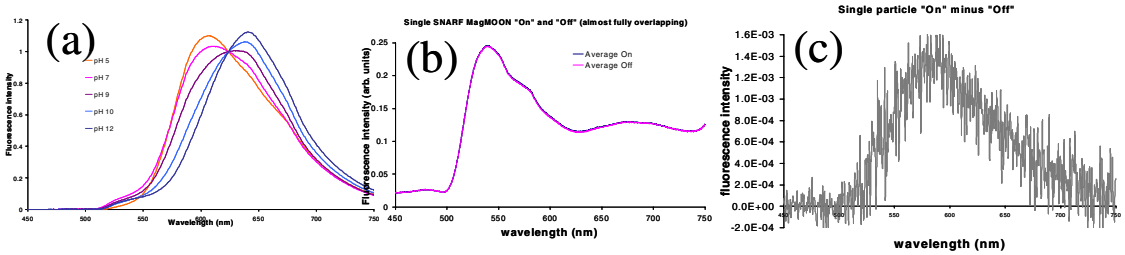

Figure 5. pH sensitive 300nm MagMOONs. (a) dependence of fluorescence from SNARF MagMOONs on pH. The spectra have been normalized to 625nm. (b) "On," "Off." (c) "On" minus "Off" spectra allows the MagMOON spectrum in acidic water to show up against the background.

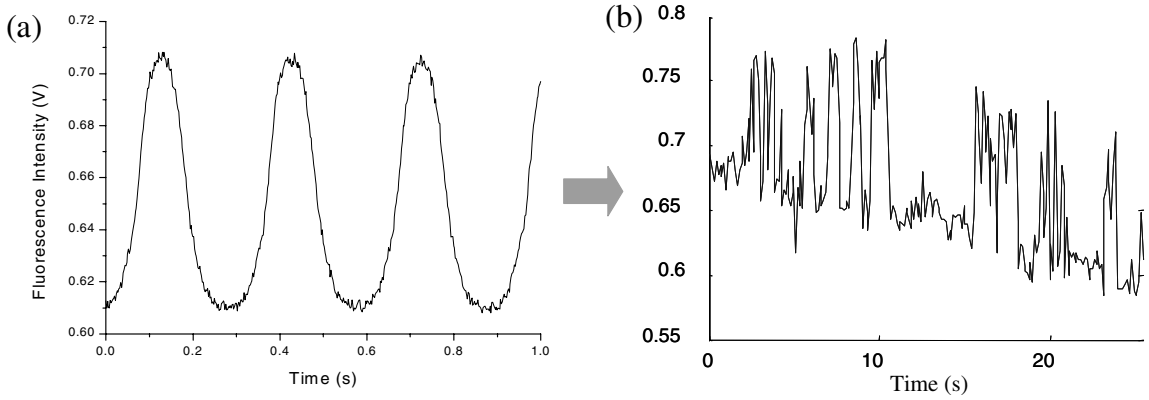

Figure 6. (a) Sinusiodal modulation of fluorescence intensity mediated by external magnetic control of MagMOON orientation. (b) In the absence of an external magnetic field, or if a MOON contains no magnetic material, the probe is modulated randomly solely due to Brownian rotation.

The preparation of Brownian MOONs, compared to that of MagMOONs, is simpler, because no embedded magnetic nano-seeds are required, as well as no external magnetic fields. Using PCA, the erratically blinking Brownian MOON spectra can be separated from constant backgrounds and other signal sources that fluctuate with different patterns in time[11].

Furthermore, the rate of fluctuation reveals information about local viscosity[10]. We note that for heterogeneous fluids the viscosity is a complex function of time scales and the size scale of the probing instrument. Large batches of metal-capped nanoparticles can be prepared with carefully chosen sizes. A number of metal-capped and moon-shaped particle preparation processes have been described [18-24]. Recently, 300nm-3μm moon shaped particles were used to observe Brownian rotation[9] and measure viscosity[10]. Similarly, 960nm moon-shaped particles were used to observe interactions with surfaces[25].

A small number of chains of two or more particles are formed during the preparation. The orientation of these chains can be tracked around all three axes allowing complete characterization of the particle orientation. These chains can be dispersed with long sonication. Rods may also be prepared to allow visualization of particle orientation around three axes[12].

Historically, the observation and theory of Brownian rotation has helped shape our views of matter. In 1828, Robert Brown observed "Brownian" rotation of relatively large aspherical pollen grains[26,27]. Einstein (1906) derived the equation for the rotational diffusion coefficient D^{rot} [28].

$$D^{rot} = RT/8\pi N_0 \eta r^3 \quad (1)$$

Where *r* is the radius of the (spherical) particle, η0 is the viscosity, T the temperature, R the gas constant and No Avogadro's number. Jean Perrin (1909) utilized this approach to determine Avogadro's number providing strong evidence for the molecular theory of matter[29]. Perrin's visual observations utilized particles approximately 10μm in diameter, with recognizable defects whose rotations could be observed. The rotational diffusion rate can be measured in terms of root mean square degrees rotated, or by the shape of the autocorrelation function of the intensity time fluctuations, for particles undergoing Brownian rotation[10,30,31]. Experiments using magnetic fields to rotate 4.4μm magnetically modulated optical nanoprobes (MagMOONs) indicated that the fluorescence intensity is proportional to the cosine of the azimuthal angle of the particles, with weaker harmonics also appearing[15]. Assuming that the fluorescence intensity from Brownian MOONs is also proportional to the cosine of the azimuthal angle, the autocorrelation function, $G^{rot}(t)$, of the fluctuations is expected to decay exponentially (equation 2)[16].

$$G^{rot}(t) = e^{-t/\tau} \quad (2a)$$

$$\tau = \kappa V \eta / 2k_B T \quad (2b)$$

For a spherical particle, the shape factor κ is 6. For aspherical particles, the shape factor depends on the relative dimensions of the particle. The rotation time depends on the volume, V, of the particle and is proportional to the viscosity of the surrounding solvent environment. If harmonics are present in the angular intensity distribution, the autocorrelation function is expected to decay more quickly. Table 1 illustrates characteristic autocorrelation decay times for several sizes of particles in solutions of different viscosity.

As is evident from the table, smaller size particles rotate rapidly allowing rapid observation of rotation. Decreasing the particle size from the 13μm particle originally used by Perrin to a 130nm particle, decreases rotation time, in the same fluid viscosity, by a factor of one million. Also, the smaller size allows one to study the local hydrodynamics for nanospheres embedded in micro- or nano-environments, i.e., the deviations from simple Brownian behavior in systems that exhibit hindered rotational motions which may characterize an interface, micelle or biological cellular compartment[30-36]. An interesting open question is the lower size limit for which the Einstein description works. We expect this limit to be in the 1-10nm range.

Table I. The rotational correlation time, τ_c, for 13, 4.4, 2, 1, .30, 0.1, 0.05 micron particles in pure water at 20°C and 37°C and 95% glycerol and pure water at 25°C and 37°C. τ_c corresponds to a root mean square rotation of 1 radian[31].

Sphere Diameter (μm)	Water 37 ºC (0.7 Pa-s)	Water 20ºC (1.0 mPa-s)	98% Glycerol 20ºC (957mPa-s)
13	9.8min	14min	9.3day
4.4	22s	32s	8.7hr
2	2.1s	3.1s	48min
1	270ms	380ms	6.1min
0.3	7.2ms	10ms	9.9s
0.1	270μs	380μs	370ms
0.05	34μs	48μs	46ms

On the microscopic scale, measurements of viscosity in the cell cytosol have varied over six orders of magnitude, depending on the size of the probe used[37]. Recent work suggests sieve-like structures within subdomains of cytoplasm that allow small particles to diffuse through while resisting the motion of larger particles[38]. In addition, liquid filled structures such as endosomes may allow particles to rotate within but not translate, causing divergence between rotational and translational brownian diffusion. Figure 7 shows Brownian MOONs reorienting within macrophage endosomal compartments. This approach allows direct observation or endosome properties and torques on the endosome, on an individual particle and endosome basis. Combined with modulated chemical sensing this method is a powerful tool for probing intracellular physiology and dynamics.

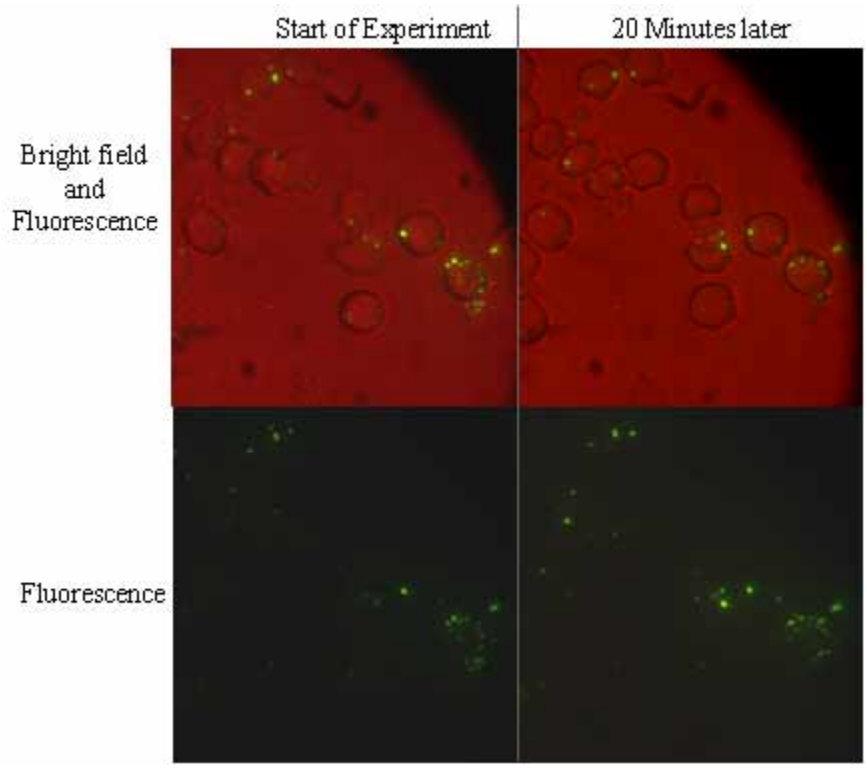

Figure 7. Top: overlaid bright field and fluorescence images showing Brownian MOONs internalized by rat macrophages at two different times, start of the experiment (left) and 20minutes later (right). Bottom: Fluorescence images of Brownian MOONs reorienting in rat Macrophages.

CONCLUSIONS:

Controlling the optical symmetry of particles produces new tools for exploration of optical, chemical, and material properties of surrounding environments. They can be used as nano-instruments such as: nanoviscometers[10,33,39,40,41], nanothermometers[42], nanobarometers, and nano-chemical sensors[1-7]. Modulation of Brownian MOONs and MagMOONs also allows the local optical, chemical, and material properties to be distinguished from the bulk properties. An example application would be for microfluidics where one could measure the local viscosity as a function of distance from surfaces of microchannels. These tools promise improved intracellular chemical imaging, high sensitivity immunoassays with simpler procedures, measuring viscosities at chosen time and size scales, and observation of vorticity in fluids, as well as simultaneous physical and chemical imaging.

ACKNOWLEDGEMENTS:

The authors gratefully acknowledge support from NSF DMR-9900434 and DARPA F49620-03-1-0297

REFERENCES

1. E. Monson *et al.*, *Biomedical Photonics Handbook*, Edited by T. Vo-Dinh (CRC Press, 2003).
2. H. A. Clark *et al.*, Mikrochimica Acta **131**(1-2), 121 (1999).
3. J. W. Aylott, Analyst **128**(4), 309 (2003).
4. H. Xu *et al.*, Analytical Chemistry **73**(17), 4124 (2001).
5. H. Xu, J. W. Aylott, and R. Kopelman, Analyst **127**(11), 1471 (2002).
6. M. Brasuel *et al.*, Analytical Chemistry **73**(10), 2221 (2001).
7. H. Xu *et al.*, Journal of Biomedical Materials Research Part a **66A**(4), 870 (2003).
8. J. N. Anker, C. Behrend, and R. Kopelman, Journal of Applied Physics **93**(10), 6698 (2003).
9. J. N. Anker and R. Kopelman, Applied Physics Letters **82**(7), 1102 (2003).
10. Behrend C.J. , Anker J.N., and Kopelman R., Applied Physics Letters (in press).
11. J. N. Anker, C. Behrend, and R. Kopelman, (In Preparation).
12. J. N. Anker, T. D. Horvath, and R. Kopelman, , European Cells and Materials **3**(Suppl. 2), 95 (2002).
13. J. F. Wang *et al.*, Science **293**(5534), 1455 (2001).
14. H. A. Clark *et al.*, Analytical Chemistry **71**(21), 4831 (1999).
15. H. Xu, J. Aylott, and R. Kopelman, Abstracts of Papers of the American Chemical Society **219**, U99 (2000).
16. K. Sasaki *et al.*, Chemistry Letters (2), 141 (1996).
17. M. Born and E. Wolf, *Principles of Optics--6th Ed, Chapter 13* (Cambridge University Press, New York, NY, 1980).
18. H. Takei and N. Shimizu, Langmuir **13**(7), 1865 (1997).
19. K. Nakahama, H. Kawaguchi, and K. Fujimoto, Langmuir **16**(21), 7882 (2000).
20. M. Himmelhaus and H. Takei, Sensors and Actuators B-Chemical **63**(1-2), 24 (2000).
21. K. Fujimoto *et al.*, Langmuir **15**(13), 4630 (1999).

22. L. A. Cameron *et al.*, Proceedings of the National Academy of Sciences of the United States of America **96**(9), 4908 (1999).

23. Y. Lu *et al.* , Journal of the American Chemical Society **125**(42), 12724 (2003).

24. J. M. Crowley, N. K. Sheridon, and L. Romano, Journal of Electrostatics **55**(3-4), 247 (2002).

25. J. Choi *et al.*, Nano Letters **3**(8), 995 (2003).

26. R. Brown, Edinburgh Phil. Journal **5**, 358 (1828).

27. R. Brown, Edinburgh J. Science **1**, 314 (1829).

28. A. Einstein, *Investigations on the Theory of the Brownian Movement* (Dover, New York, N. Y., 1956).

29. J Perrin, *Brownian Movement and Molecular Reality* (Taylor and Francis, 1910).

30. G. H. Koenderink, *Rotational and Translational Diffusion in Colloidal Mixtures* (Cip-Gegevens Koninklikjke Bibliotheek, Dan Haag, Netherlands, 2003).

31. P. A. Valberg and J. P. Butler, Biophysical Journal **52**(4), 537 (1987).

32. M. Tomishige, Y. Sako, and A. Kusumi, Journal of Cell Biology **142**(4), 989 (1998).

33. F. C. Mackintosh and C. F. Schmidt, Current Opinion in Colloid & Interface Science **4**(4), 300 (1999).

34. T. Gisler and D. A. Weitz, Current Opinion in Colloid & Interface Science **3**(6), 586 (1998).

35. F. H. C. Crick and A. F. W. Hughes (1950), Vol. 37.

36. K. Luby-Phelps, Vol. 192, pp. 189-221.

37. P. A. Valberg and H. A. Feldman, Biophysical Journal **52**(4), 551 (1987).

38. L. W. Janson, K. Ragsdale, and K. Lubyphelps, Biophysical Journal **71**(3), 1228 (1996).

39. Y. Nicolas *et al.* , Food Hydrocolloids **17**, 907 (2003).

40. V. Breedveld and D. J. Pine, Journal of Materials Science, **38**, 4461 (2003).

41. K. J. Van Vliet, G. Bao, and S. Suresh, Acta Materialia, **51** 5881 (2003).

42. O. Zohar *et al.* , Biophysical Journal, **74**(1), 82 (1998).